

Novel Dynamical Magnetolectric Effects in Multiferroic BiFeO₃

S. Omid Sayedaghaee,^{1,2} Bin Xu,^{1,3} Sergey Prosandeev,^{1,4} Charles Paillard,^{1,5} and L. Bellaïche¹

¹Physics Department and Institute for Nanoscience and Engineering, University of Arkansas, Fayetteville, Arkansas 72701, USA

²Microelectronics-Photonics Program, University of Arkansas, Fayetteville, Arkansas 72701, USA

³School of Physical Science and Technology, Soochow University, Suzhou, Jiangsu 215006, China

⁴Institute of Physics and Physics Department of Southern Federal University, Rostov-na-Donu 344090, Russia

⁵Laboratoire Structures, Propriétés et Modélisation des Solides, CentraleSupélec, CNRS UMR 8580, Université Paris-Saclay, 91190 Gif-sur-Yvette, France

 (Received 10 October 2018; revised manuscript received 19 January 2019; published 7 March 2019)

An atomistic effective Hamiltonian scheme is employed within molecular dynamics simulations to investigate how the electrical polarization and magnetization of the multiferroic BiFeO₃ respond to time-dependent ac magnetic fields of various frequencies, as well as to reveal the frequency dependency of the dynamical (quadratic) magnetolectric coefficient. We found the occurrence of vibrations having phonon frequencies in both the time dependency of the electrical polarization and magnetization (for any applied ac frequency), therefore making such vibrations of electromagnonic nature, when the homogeneous strain of the system is frozen (case 1). Moreover, the quadratic magnetolectric coupling constant is monotonic and almost dispersionless in the sub-THz range in this case 1. In contrast, when the homogeneous strain can fully relax (case 2), two additional low-frequency and strain-mediated oscillations emerge in the time-dependent behavior of the polarization and magnetization, which result in resonances in the quadratic magnetolectric coefficient. Such additional oscillations consist of a mixing between acoustic phonons, optical phonons, and magnons, and reflect the existence of a new quasiparticle that can be coined an “electroacoustic magnon.” This latter finding can prompt experimentalists to shape their samples to take advantage of, and tune, the magnetostrictive-induced mechanical resonance frequency, in order to achieve large dynamical magnetolectric couplings.

DOI: [10.1103/PhysRevLett.122.097601](https://doi.org/10.1103/PhysRevLett.122.097601)

Multiferroic materials can exhibit a magnetolectric (ME) coupling between their electrical and magnetic moments. Such a coupling is promising for designing novel devices by controlling magnetization with electric fields, or conversely, electrical polarization with magnetic fields [1–6]. Two paths can be taken to realize this magnetolectric coupling: direct coupling of polarization with a magnetic field versus mediated by strain. The latter is particularly investigated by mixing efficient magnetostrictive and piezoelectric materials, in composites [7] or heterostructures [8,9].

These two types of coupling have been mostly for static properties [1–4,10,11]. In other words, how strain affects dynamical properties of multiferroics is mostly an uncharted territory. In particular, it is yet unclear whether ME coefficients can be improved with mechanical resonances in single phase materials, as in laminar composites [8,12]. It is also legitimate to investigate the effect of strain on electromagnons (mixing of phonons and magnons [13–16]), or even on the formation of a novel type of (dynamical) object.

To resolve such issues, we (1) conducted molecular dynamics (MD) simulations within an effective Hamiltonian scheme on BiFeO₃ (BFO), a prototypical multiferroic, subject to ac magnetic fields; and (2) monitored the resulting time dependency of its electrical polarization and

magnetization. It is found, that (i) electromagnons (of phonon frequencies) exist independently of allowing the homogeneous strain to relax; and (ii) relaxation of the homogeneous strain results in the emergence of a new type of quasiparticle consisting of acoustic vibrations coupled to phonons and magnons, and generating resonances in the quadratic ME coefficient.

Here, we use the effective Hamiltonian (H_{eff}) scheme of BiFeO₃ described in Ref. [17]. Its total energy $E_{\text{BFO}}(\{\mathbf{u}_i\}, \{\eta_l\}, \{\omega_i\}, \{\mathbf{m}_i\})$ includes four types of degrees of freedom: (1) the local modes $\{\mathbf{u}_i\}$, proportional to the local electric dipoles [18,19]; (2) the homogeneous $\{\eta_l\}$ and inhomogeneous $\{\eta_l\}$ strain tensors [18,19]; (3) the pseudovectors $\{\omega_i\}$ that characterize the oxygen octahedral tiltings [20] (also called antiferrodistortive (AFD) motions); and (4) the magnetic moments $\{\mathbf{m}_i\}$ of the Fe ions (in all cases, the subscript i labels unit cells in our simulated supercells). The total energy of H_{eff} for BFO is a sum of three main energies $E^{\text{tot}} = E^{\text{FE}}(\{\mathbf{u}_i\}, \{\eta_l\}) + E^{\text{AFD}}(\{\mathbf{u}_i\}, \{\eta_l\}, \{\omega_i\}) + E^{\text{MAG}}(\{\mathbf{m}_i\}, \{\mathbf{u}_i\}, \{\eta_l\}, \{\omega_i\})$, where $\{\eta_l\}$ is the total strain tensor (i.e., that incorporates both the homogenous and inhomogeneous components). E^{FE} is the energy involving the local modes and elastic deformations, while E^{AFD} is the energy that gathers the AFD motions and

their couplings with local modes and strains. Moreover, E^{MAG} contains the magnetic degrees of freedom and their couplings with local modes, AFD tiltings, and strains, and reads [21]

$$\begin{aligned}
 E^{\text{MAG}} = & \sum_{ij\alpha\gamma} Q_{ij\alpha\gamma} m_{i\alpha} m_{j\gamma} + \sum_{ij\alpha\gamma} S_{ij\alpha\gamma} m_{i\alpha} m_{j\gamma} \\
 & + \sum_{ij,\alpha\gamma\nu\delta} E_{ij,\alpha\gamma\nu\delta} m_{i\alpha} m_{j\gamma} u_{i\nu} u_{j\delta} \\
 & + \sum_{ij,\alpha\gamma\nu\delta} F_{ij,\alpha\gamma\nu\delta} m_{i\alpha} m_{j\gamma} \omega_{i\nu} \omega_{j\delta} \\
 & + \sum_{ijl,\alpha\gamma} G_{ijl,\alpha\gamma} \eta_l(i) m_{i\alpha} m_{j\gamma} \\
 & + \sum_{ij} L_{ij} (\boldsymbol{\omega}_i - \boldsymbol{\omega}_j) \cdot (\mathbf{m}_i \times \mathbf{m}_j), \quad (1)
 \end{aligned}$$

where $\alpha, \gamma, \nu, \delta$ denote the Cartesian components, and the indices i and j run over sites. The six terms of Eq. (1) are, respectively, the dipolar interactions between the magnetic moments, the short-range magnetic exchange coupling, the coupling between the magnetic moments with local modes, AFD motions and strain, and a particular Dzyaloshinskii-Moriya (DM) interaction involving the oxygen octahedral tiltings. Under a magnetic field, an additional term $-\sum_i \mathbf{m}_i \cdot \mathbf{H}$ is also incorporated into the total energy. This effective Hamiltonian is then adopted for MD simulations, by solving the equations of motion for local modes, oxygen octahedral tilting, strains, and magnetic moments, as detailed in Refs. [22–24]. We adopt a $12 \times 12 \times 12$ supercell in terms of the 5-atom perovskite unit cell, with periodic boundary conditions. MD simulations are carried out at 1 K under the NPT ensemble when the homogeneous strain can relax during the simulations versus the NVT ensemble when the total strain is frozen during the computations. More details about the MD computations and the effective Hamiltonian schemes for BFO are given in the Supplemental Material [21,25–37].

We apply to our considered state of BFO a magnetic field with two components, both aligned along the $[11\bar{2}]$ direction: a dc field of magnitude $H_{\text{dc}} = 245$ T and an ac field given by $h_{\text{ac}} \sin(\omega t)$ where $h_{\text{ac}} = 61.2$ T and $\nu = \omega/2\pi$ is the frequency of the applied ac magnetic field. These fields are chosen to have high magnitude to numerically observe the response of polarization since ME coefficients are known to be rather small in BiFeO_3 [21,32,38,39].

Let us first restrict ourselves to the case when the homogeneous strain is not allowed to relax (therefore adopting the homogeneous strain of the $R3c$ state under a sole dc magnetic field of 245 T) during the MD simulations—while the inhomogeneous strain can still vary. Figure 1(a) depicts the temporal behavior of the component of the polarization along the $[111]$ direction in the $R3c$ phase for a frequency (ν) of 160 GHz. Moreover, Fig. 1(b) displays the corresponding Fourier transform, and

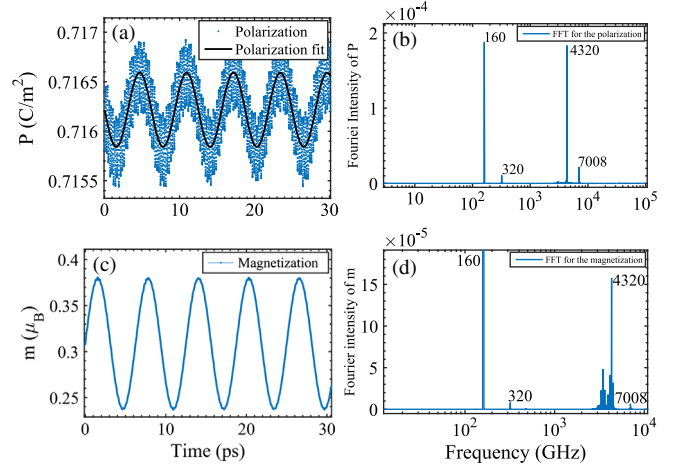


FIG. 1. Temporal evolution of the polarization [panel (a)] and magnetization [panel (c)] in BiFeO_3 under a dc magnetic field of 245 T of magnitude coexisting with an ac magnetic field of 61.2 T of magnitude and of 160 GHz of frequency, along with their resulting Fourier transforms [panels (b) and (d), respectively] as a function of frequency, in the case that the homogeneous strain is frozen in the MD simulations. The dc and ac magnetic fields are applied along the $[11\bar{2}]$ direction. The displayed polarization is along the $[111]$ direction while the magnetization is along the $[11\bar{2}]$ direction. The solid line in panel (a) represents the fit of the MD data by a function of the form $A + B \sin \omega t$ where $\omega/2\pi = 160$ GHz.

demonstrates that four main frequencies govern the temporal evolution of the electrical polarization: the applied ac frequency and its double (i.e., 160 and 320 GHz), which reveals the occurrence of *dynamical* magnetoelectric effects, and two higher frequencies that are of the order of 4300 and 7000 GHz, which are natural *phonon* frequencies (see Refs. [22,26,40–47]).

Interestingly and as evidenced in Fig. 1(d), these four frequencies also appear in the Fourier transform of the curve representing the component of the magnetization along the $[11\bar{2}]$ direction as a function of time [shown in Fig. 1(c)]. The frequency of 160 GHz seen in Fig. 1(d) emerges from the energy coupling the magnetic moment with the ac magnetic field, while the frequency at 320 GHz is characteristic of nonlinear magnetic couplings. Remarkably, the high frequencies around 4300 GHz seen in Fig. 1(d), and at lesser extent at 7000 GHz, reveal that natural phonons mix with magnons and affect the temporal evolution of the magnetization under a time-dependent magnetic field. Natural phonons thus become electromagnons [14–16], consistent with Ref. [48] for the $R3c$ phase of BiFeO_3 —these electromagnons are presently numerically found to originate from the fact that polarization and oxygen octahedral tiltings affect the magnetic exchange parameters [third and fourth terms of Eq. (1)]. Note that magnons having frequencies smaller than 160 GHz are not seen in Fig. 1(d) because the applied magnetic fields are too large and thus force the magnetic moments to mostly follow

them, in addition to possessing smaller oscillations arising from the coupling of the magnetic moments with the aforementioned phonons [see Fig. 1(c)].

Let us now allow the homogeneous and inhomogeneous strains to fully relax during the MD simulations, and determine how it affects the temporal evolutions of the polarization and magnetization [see Figs. 2(a) and 2(c), respectively], as well as their Fourier transforms [cf. Figs. 2(b) and 2(d), respectively]. Figures 2(e) and 2(f) further report the variation of the diagonal elements of the homogeneous strain tensor ($\eta_{H,1}$, $\eta_{H,2}$, and $\eta_{H,3}$) as a function of time and of their Fourier transforms, respectively, while Figs. 2(g) and 2(h) provide similar information but for the shear elements of the homogeneous strain tensor ($\eta_{H,4}$, $\eta_{H,5}$, and $\eta_{H,6}$).

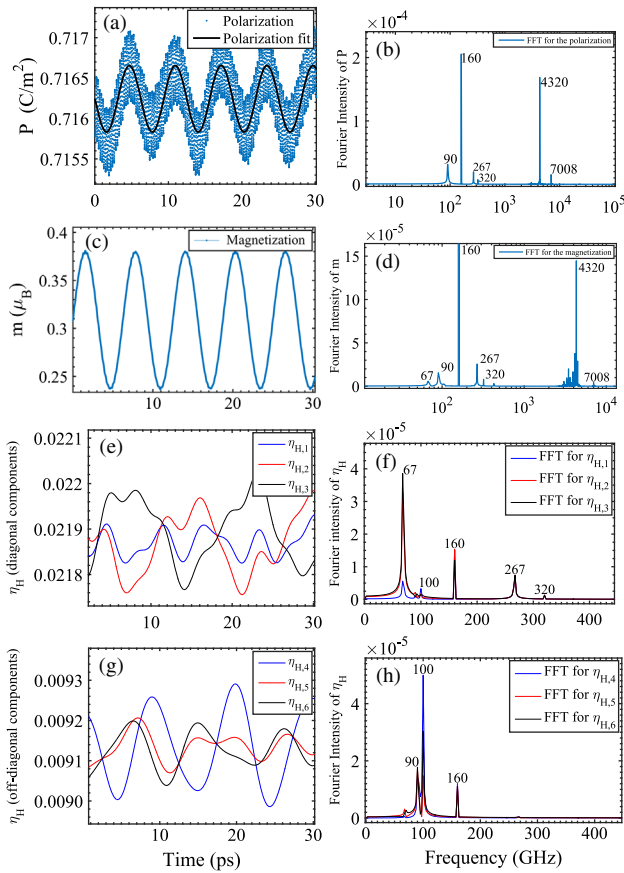


FIG. 2. Temporal evolution of the polarization [panel (a)], magnetization [panel (c)], diagonal elements of the homogeneous strain tensor [panel (e)], and shear elements of the homogeneous strain tensor [panel (g)] in BiFeO_3 under a dc magnetic field of 245 T of magnitude coexisting with an ac magnetic field of 61.2 T of magnitude and of 160 GHz of frequency, along with their resulting Fourier transforms [panels (b), (d), (f), and (h), respectively] as a function of frequency, when the homogeneous strain is allowed to relax during the MD simulations. The dc and ac magnetic fields are applied along the $[11\bar{2}]$ direction. The displayed polarization is along the $[111]$ direction while the magnetization is along the $[11\bar{2}]$ direction.

Remarkably, allowing the homogeneous strain to relax generates two *additional* frequencies in the Fourier transform of the polarization-versus-time curve with respect to the case of fixed homogeneous strains. These two frequencies are about 90 and 267 GHz, respectively, and can also be seen in the Fourier transform of the magnetization-versus-time functions. Figure 2(h) reveals that the frequency of 90 GHz originates from the oscillations of the shear elements of $\eta_{H,4}$, $\eta_{H,5}$, and $\eta_{H,6}$, while that of 267 GHz can be traced back to the vibrations of the diagonal ($\eta_{H,1}$, $\eta_{H,2}$, and $\eta_{H,3}$) elements of the homogeneous strain according to Fig. 2(f). Figures 2(f) and 2(h) further indicate that the diagonal and shear elements of the homogeneous strain tensor adopt the frequency of the applied magnetic fields of 160 GHz too, and that $\eta_{H,1}$, $\eta_{H,2}$, and $\eta_{H,3}$ also possess another frequency of the order of 67 GHz that slightly appears in the Fourier transform of the magnetization as shown in Fig. 2(d) (note that, on the other hand, we did not find any frequency higher than 320 GHz in the Fourier transforms of all homogeneous strain components, including the phonon frequencies). Comparing the results between the cases of the fixed versus relaxed homogeneous strain therefore demonstrates that, in our simulations, the homogeneous strain tensor has its own natural frequencies of the order of 90 and 267 GHz that then couple with oscillations of both the polarization and magnetization [Note that these two frequencies are indeed natural frequencies of the homogeneous strain because they are also numerically found (not shown here) in the Fourier transform of the homogeneous strain when only a dc magnetic field is applied or even when no magnetic field is imposed on BFO, with the homogeneous strain having the possibility to relax during all these additional simulations]. In other words, one can create a new type of quasiparticle mixing acoustic phonons, optical phonons, and magnons, when applying ac magnetic fields with specific frequencies (i.e., 90 and 267 GHz here). Such creation of this quasiparticle can be understood as follows: the magnetic field at these frequencies naturally activates magnons, via the direct interaction between magnetic field and magnetic moments, which in turn dynamically couple with the strain and its natural frequencies via the magnetostrictive effect. This dynamical strain then activates optical phonons at these frequencies, because of couplings between strain and electrical dipoles (via electrostrictive and piezoelectric effects), therefore resulting in the formation of this quasiparticle. We propose to name such a quasiparticle “electroacoustic magnon” to emphasize that, unlike “traditional” electromagnons, strain also plays a role in their creation. Note that pump-probe experiments revealed acoustic excitations having similar frequencies as our predicted electroacoustic magnons, namely, around 30 and 50 GHz for transverse and longitudinal acoustic modes in BFO, respectively [49,50] (note also that the presently calculated natural frequencies of the

electroacoustic magnons naturally depend on the choice of the homogeneous strain mass adopted in our MD simulations). Moreover, a peak at about 300 GHz has been observed in the Raman spectrum of the spin-canted magnetic structure of epitaxial BFO films [36]. Furthermore, a phenomenon analogous to our proposed electroacoustic magnons has just been reported in Ref. [51], that is a dynamical coupling between nuclear spins and electromechanical phonons. Such a phenomenon consists of applying an ac electric field at the natural frequency of a resonator, which leads to an electrically tunable phonon that imparts diagonal and shear strains oscillating with time and which then dynamically couple with spins of nuclei (via a quadruple interaction between strains and spins there). This resulting dynamical coupling between spins and electromechanical phonons was indicated to open up quantum state engineering, such as coherent coupling between sound and nuclei and mechanical cooling of solid-state nuclei [51]. Such interesting possibilities therefore hint that our presently discovered electroacoustic magnons may lead to novel and important devices.

Let us now reveal how these electroacoustic magnons affect the dynamical magnetoelectric coefficients. For that, let us first recall the following equation of any component i of the polarization under magnetic fields [52,53]: $P_i = P_i^s + \alpha_{ij}H_j + \frac{1}{2}\beta_{ijk}H_jH_k$, in which P_i^s is the i component of the spontaneous polarization, while H_j and H_k are components of the magnetic field. Moreover, α_{ij} and β_{ijk} are linear and quadratic magnetoelectric coefficients, respectively. Assuming that the linear ME coefficient is negligible compared to the quadratic coefficient (as suggested in Refs. [21,54] for large fields) leads to the following equation for the polarization (along the [111] direction) when applying a magnetic field (along the [112] direction) $H = H_{dc} + h_{ac}e^{i(\omega t - (\pi/2))}$:

$$P(t) = P_0 + \beta(0, \omega)H_{dc}h_{ac}e^{i[\omega t - (\pi/2)]} + \beta(\omega, \omega)\frac{1}{2}h_{ac}^2e^{i(2\omega t - \pi)}. \quad (2)$$

The second and third terms on the right-hand side of Eq. (2) characterize the magnetic-field induction of a polarization component with the same frequency of applied ac magnetic field and a second harmonic generation, respectively—which explains the occurrence of a strong Fourier transform at 160 GHz and a weaker one at 320 GHz in Figs. 1(b) and 1(d). Note that Fig. 1(a) also shows the fit of $P(t)$ by a function of the form $A + B \sin \omega t$ by means of a solid line. Such a fit nicely goes throughout the numerical MD data, therefore implying that (i) the linear ME coefficient and $\beta(\omega, \omega)$ can be neglected in front of $\beta(0, \omega)$ for the ac frequency of 160 GHz (the deviation of the MD data with respect to the fit consists of rapid oscillations associated with the phonon frequencies of about 4300 and 7000 GHz); and (ii) the validity of Eq. (2) is confirmed by our MD data.

Taking now into account that $\beta(0, \omega)$ is a complex number (especially close to resonant frequencies) we rewrite $\beta(0, \omega) = \beta'(0, \omega) + i\beta''(0, \omega)$, whose separate contributions can be computed thanks to Eq. (2) via

$$\beta'(0, \omega) = \frac{\frac{2}{L} \int_0^L (P(t) - P_0) \sin \omega t dt}{H_{dc}h_{ac}}$$

$$\beta''(0, \omega) = \frac{\frac{2}{L} \int_0^L (P(t) - P_0) \cos \omega t dt}{H_{dc}h_{ac}}, \quad (3)$$

where L is the overall simulation time.

We now apply, in addition to the dc magnetic field of 245 T, ac magnetic fields of the same magnitude of 61.2 T as in Figs. 1 and 2 but of different frequencies ranging between 20 GHz and 500 GHz (both fields were applied along [112]). Using Eqs. (3), $\beta(0, \omega)$ is determined in the frozen [Fig. 3(a)] and relaxed [Fig. 3(b)] homogeneous strain cases. When the homogeneous strain is fixed in the simulations, the imaginary part of $\beta(0, \omega)$ is basically null for any ac frequency while the real part $\beta'(0, \omega)$ is nearly independent of the frequency taking a value of about $2.0 \times 10^{-8} \text{ C/m}^2\text{T}^2 = 0.32 \times 10^{-19} \text{ s/A}$ in magnitude—that agrees very well with the β_{311} coefficient of $0.3 \times 10^{-19} \text{ s/A}$ measured in Ref. [39]. On the other hand, when the homogeneous strain fully relaxes, $\beta(0, \omega)$ exhibits two resonances at precisely the two frequencies of the electroacoustic magnons, as evidenced by strong peaks of the $\beta''(0, \omega)$ imaginary part at 90 and 267 GHz that are accompanied by strong negative values immediately followed by strong positive values of the $\beta'(0, \omega)$ real part in the near vicinity of these two frequencies. Relaxing the homogeneous strain has thus dramatic consequences on the dynamical quadratic ME coefficients near some resonant frequencies because such strain dynamically couples with both the polarization and magnetization. The divergences of $\beta(0, \omega)$ at these two resonances that are induced by indirect (i.e., strain mediated) ME coupling therefore differ in nature from the divergences of the linear dynamical ME coefficient predicted to occur at magnons or phonon

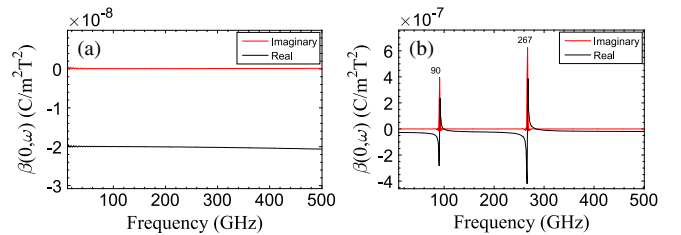


FIG. 3. Dependency of the real and imaginary parts of the $\beta(0, \omega)$ dynamical quadratic ME coefficient on the frequency of the ac applied magnetic field when the homogeneous strain is frozen [panel (a)] versus when the homogeneous strain can relax in the MD simulations [panel (b)].

frequencies in Ref. [55] since the latter originate from a *direct* coupling between polarization and magnetism. Note that electromechanically mediated resonance in magneto-electric coefficients was already observed in laminar piezo-electric-magneto-electric composite structures [8,12]. Here, it is of interest in the design of magneto-electric based sensors, for which the resonance frequency can be tuned by properly designing the shape and size of a *single phase* material (such as BiFeO₃).

Note also that we are unable to extract $\beta(0, \omega)$ for high frequencies, because the time dependency of the polarization becomes noisy due to interference between the phonon frequencies and the applied magnetic field frequency. This explains why we limited ourselves to frequencies up to 500 GHz in Fig. 3 and prevents us from checking if $\beta(0, \omega)$ has also resonances at the phonon or electromagnon frequencies of about 4300 and 7000 GHz.

In summary, molecular dynamics effective Hamiltonian simulations predicting the response of the polarization and magnetization to time-dependent magnetic fields of different ac frequencies allowed us to extract the dispersion of the quadratic ME coefficient up to 500 GHz. In particular, electromagnons having phonon frequencies are found whether the homogeneous strain is frozen or relaxed during the simulations. The reported strain-mediated resonances in the magneto-electric coupling are of large interest to design devices with proper shape of the sample for dynamical applications, since such shape can tune the resonant mechanical frequencies [56]. Those resonances can be described by a new type of quasiparticle that we coin “electroacoustic magnon,” which arises when the frequency of the ac magnetic field resonantly excites homogeneous strain modes. This quasiparticle consists of a mixing of acoustic phonon, optical phonon, and magnon. The calculations reported in this Letter were done at very low temperature and high magnitude of the magnetic fields in order to have less fluctuation of the order parameters (e.g., polarization and magnetization)—yielding less numerical noise and thus better accuracy for the magneto-electric response. However, as shown in the Supplemental Material [37], our findings (e.g., resonances in the quadratic magneto-electric coefficients originating from our discovered electroacoustic magnons) still qualitatively hold at 300 K and also for smaller magnetic fields. We strongly believe that these results are not only relevant to BiFeO₃ but rather to many multiferroics due to couplings between polarization, magnetization, and strains in such systems. We thus hope that the present results deepen the current knowledge of multiferroics, in general, and of dynamical magneto-electric effects, in particular.

S. O. S. and L. B. thank the DARPA Grant No. HR0011-15-2-0038 (under the MATRIX program). B. X. acknowledges funding from Air Force Office of Scientific Research under Grant No. FA9550-16-1-0065. S. P. thanks ONR Grant No. N00014-17-1-2818. C. P. acknowledges the

ARO Grant No. W911NF-16-1-0227. Some computations were also made possible owing to MRI Grant No. 0722625 from NSF, ONR Grant No. N00014-15-1-2881 (DURIP), and a Challenge grant from the Department of Defense. S. P. also appreciates support of Russian Ministry of Science and Education (RMES) 3.1649.2017/4.6 and RFBR 18-52-00029_Bel_a. B. X. also thanks support from Priority Academic Program Development (PAPD) of Jiangsu Higher Education Institutions. The authors thank R. de Sousa and S. Kamba for insightful discussions about electromagnons.

-
- [1] T. Zhao, A. Scholl, F. Zavaliche, K. Lee, M. Barry, A. Doran, M. P. Cruz, Y. H. Chu, C. Ederer, N. A. Spaldin, R. R. Das, D. M. Kim, S. H. Baek, C. B. Eom, and R. Ramesh, *Nat. Mater.* **5**, 823 (2006).
 - [2] D. Lebeugle, D. Colson, A. Forget, M. Viret, A. M. Bataille, and A. Gukasov, *Phys. Rev. Lett.* **100**, 227602 (2008).
 - [3] W. Eerenstein, N. D. Mathur, and J. F. Scott, *Nature (London)* **442**, 759 (2006).
 - [4] M. Fiebig, T. Lottermoser, D. Frhlich, A. V. Goltsev, and R. V. Pisarev, *Nature (London)* **419**, 818 (2002).
 - [5] N. Hur, S. Park, P. A. Sharma, J. S. Ahn, S. Guha, and S. W. Cheong, *Nature (London)* **429**, 392 (2004).
 - [6] T. Lottermoser, T. Lonkai, U. Amann, D. Hohlwein, J. Ihringer, and M. Fiebig, *Nature (London)* **430**, 541 (2004).
 - [7] N. Ortega, A. Kumar, J. F. Scott, and R. S. Katiyar, *J. Phys. Condens. Matter* **27**, 504002 (2015).
 - [8] C. Popov, H. Chang, P. M. Record, E. Abraham, R. W. Whatmore, and Z. Huang, *J. Electroceram.* **20**, 53 (2008).
 - [9] P.-E. Janolin, N. A. Pertsev, D. Sichuga, and L. Bellaiche, *Phys. Rev. B* **85**, 140401(R) (2012).
 - [10] J.-M. Hu, L.-Q. Chen, and C.-W. Nan, *Adv. Mater.* **28**, 15 (2016).
 - [11] V. Garcia, M. Bibes, and A. Barthélémy, *C.R. Phys.* **16**, 168 (2015).
 - [12] U. Laletsin, N. Padubnaya, G. Srinivasan, and C. P. Devreugd, *Appl. Phys. A* **78**, 33 (2004).
 - [13] G. Smolenskii and I. Chupis, *Sov. Phys. Usp.* **25**, 475 (1982).
 - [14] M. Cazayous, Y. Gallais, A. Sacuto, R. de Sousa, D. Lebeugle, and D. Colson, *Phys. Rev. Lett.* **101**, 037601 (2008).
 - [15] A. B. Sushkov, M. Mostovoy, R. Valdes Aguilar, S.-W. Cheong, and H. D. Drew, *J. Phys. Condens. Matter* **20**, 434210 (2008).
 - [16] R. Valdés Aguilar, M. Mostovoy, A. B. Sushkov, C. L. Zhang, Y. J. Choi, S.-W. Cheong, and H. D. Drew, *Phys. Rev. Lett.* **102**, 047203 (2009).
 - [17] S. Prosandeev, D. Wang, W. Ren, J. Íñiguez, and L. Bellaiche, *Adv. Funct. Mater.* **23**, 234 (2013).
 - [18] W. Zhong, D. Vanderbilt, and K. M. Rabe, *Phys. Rev. Lett.* **73**, 1861 (1994).
 - [19] W. Zhong, D. Vanderbilt, and K. M. Rabe, *Phys. Rev. B* **52**, 6301 (1995).
 - [20] I. A. Kornev, L. Bellaiche, P. E. Janolin, B. Dkhil, and E. Suard, *Phys. Rev. Lett.* **97**, 157601 (2006).
 - [21] D. Albrecht, S. Lisenkov, W. Ren, D. Rahmedov, I. A. Kornev, and L. Bellaiche, *Phys. Rev. B* **81**, 140401 (2010).

- [22] D. Wang, J. Weerasinghe, and L. Bellaïche, *Phys. Rev. Lett.* **109**, 067203 (2012).
- [23] S. Bhattacharjee, D. Rahmedov, D. Wang, J. Íñiguez, and L. Bellaïche, *Phys. Rev. Lett.* **112**, 147601 (2014).
- [24] K. Patel, S. Prosandeev, and L. Bellaïche, *npj Comput. Mater.* **3**, 34 (2017).
- [25] D. J. Evans, W. G. Hoover, B. H. Failor, B. Moran, and A. J. C. Ladd, *Phys. Rev. A* **28**, 1016 (1983).
- [26] R. Haumont, J. Kreisel, P. Bouvier, and F. Hippert, *Phys. Rev. B* **73**, 132101 (2006).
- [27] J. B. Neaton, C. Ederer, U. V. Waghmare, N. A. Spaldin, and K. M. Rabe, *Phys. Rev. B* **71**, 014113 (2005).
- [28] I. C. Infante, S. Lisenkov, B. Dupé, M. Bibes, S. Fusil, E. Jacquet, G. Geneste, S. Petit, A. Courtial, J. Juraszek, L. Bellaïche, A. Barthélémy, and B. Dkhil, *Phys. Rev. Lett.* **105**, 057601 (2010).
- [29] D. Rahmedov, D. Wang, J. Íñiguez, and L. Bellaïche, *Phys. Rev. Lett.* **109**, 037207 (2012).
- [30] M. Ramazanoglu, W. Ratcliff, Y. J. Choi, S. Lee, S.-W. Cheong, and V. Kiryukhin, *Phys. Rev. B* **83**, 174434 (2011).
- [31] M. Ramazanoglu, M. Laver, W. Ratcliff, S. M. Watson, W. C. Chen, A. Jackson, K. Kothapalli, S. Lee, S.-W. Cheong, and V. Kiryukhin, *Phys. Rev. Lett.* **107**, 207206 (2011).
- [32] Y. F. Popov, A. K. Zvezdin, G. P. Vorbev, V. A. Murashev, and D. N. Racov, *JETP Lett.* **57**, 65 (1993).
- [33] Y. F. Popov, A. Kadomtseva, G. Vorob'ev, and A. Zvezdin, *Ferroelectrics* **162**, 135 (1994).
- [34] M. Tokunaga, M. Azuma, and Y. Shimakawa, *J. Phys. Soc. Jpn.* **79**, 064713 (2010).
- [35] A. Agbelele, D. Sando, C. Toulouse, C. Paillard, R. John-son, R. Ruffer, A. Popkov, C. Carrétero, P. Rovillain, J.-M. Le Breton *et al.*, *Adv. Mater.* **29**, 1602327 (2017).
- [36] D. Sando *et al.*, *Nat. Mater.* **12**, 641 (2013).
- [37] See Supplemental Material at <http://link.aps.org/supplemental/10.1103/PhysRevLett.122.097601> for more details about the effective Hamiltonian method used and the Molecular Dynamics (MD) calculations as well as the results of additional calculations conducted at 300K or for different magnetic fields.
- [38] S. Lisenkov, I. A. Kornev, and L. Bellaïche, *Phys. Rev. B* **79**, 012101 (2009); **79**, 219902(E) (2009).
- [39] C. Tabares-Munoz, J. P. Rivera, A. Bezinges, A. Monnier, and H. Schmid, *Jpn. J. Appl. Phys.* **24**, 1051 (1985).
- [40] S. Kamba, D. Nuzhnyy, M. Savinov, J. Sebek, J. Petzelt, J. Prokleska, R. Haumont, and J. Kreisel, *Phys. Rev. B* **75**, 024403 (2007).
- [41] H. Fukumura, S. Matsui, H. Harima, T. Takahashi, T. Itoh, K. Kisoda, M. Tamada, Y. Noguchi, and M. Miyayama, *J. Phys. Condens. Matter* **19**, 365224 (2007).
- [42] R. P. S. M. Lobo, R. L. Moreira, D. Lebeugle, and D. Colson, *Phys. Rev. B* **76**, 172105 (2007).
- [43] D. Rout, K.-S. Moon, and S.-J. L. Kang, *J. Raman Spectrosc.* **40**, 618 (2009).
- [44] J. Lu, M. Schmidt, P. Lunkenheimer, A. Pimenov, A. A. Mukhin, V. D. Travkin, and A. Loidl, *J. Phys. Conf. Ser.* **200**, 012106 (2010).
- [45] R. Palai, H. Schmid, J. F. Scott, and R. S. Katiyar, *Phys. Rev. B* **81**, 064110 (2010).
- [46] A. A. Porporati, K. Tsuji, M. Valant, A.-K. Axelsson, and G. Pezzotti, *J. Raman Spectrosc.* **41**, 84 (2010).
- [47] J. Hlinka, J. Pokorny, S. Karimi, and I. M. Reaney, *Phys. Rev. B* **83**, 020101(R) (2011).
- [48] C.-M. Chang, B. K. Mani, S. Lisenkov, and I. Ponomareva, *Ferroelectrics* **494**, 68 (2016).
- [49] M. Lejman, G. Vaudel, I. C. Infante, I. Chaban, T. Pezeril, M. Edely, G. F. Nataf, J. Kreisel, V. E. Gusev, B. Dkhil, and P. Ruello, *Nat. Commun.* **5**, 4301 (2014).
- [50] M. Lejman, G. Vaudel, I. C. Infante, P. Gemeiner, V. E. Gusev, B. Dkhil, and P. Ruello, *Nat. Commun.* **7**, 12345 (2016).
- [51] Y. Okazaki, I. Mahboob, K. Onomitsu, S. Sasaki, S. Nakamura, N. Kaneko, and H. Yamaguchi, *Nat. Commun.* **9**, 2993 (2018).
- [52] H. Schmid, *Int. J. Magn.* **4**, 337 (1973).
- [53] M. Fiebig, *J. Phys. D: Appl. Phys.* **38**, 123 (2005).
- [54] I. A. Kornev, S. Lisenkov, R. Haumont, B. Dkhil, and L. Bellaïche, *Phys. Rev. Lett.* **99**, 227602 (2007).
- [55] K. L. Livesey and R. L. Stamps, *Phys. Rev. B* **81**, 094405 (2010).
- [56] Note that the homogeneous strain tensor is a degree of freedom in our molecular dynamics simulations and is thus assigned a mass for its equation of motion. Consequently, it has its own natural frequencies in the infinite BiFeO₃ crystal, which is our presently studied system (this fact is numerically confirmed by varying this mass, which results in the shift of the mechanical and thus “electroacoustic magnon” frequencies). What is interesting is that mechanical frequencies are known to be practically dependent on the sample size. As a result, alternating the sample size should allow us to control the frequencies of our discovered electroacoustic magnons.